

RESTRICTED

NACA RM No. L7L12



19 APR 1948 UNCLASSIFIED

NACA

RESEARCH MEMORANDUM

MEASUREMENTS OF THE WING AND TAIL LOADS
DURING THE ACCEPTANCE TESTS OF
BELL XS-1 RESEARCH AIRPLANE

By

De E. Beeler and John P. Mayer

Langley Memorial Aeronautical Laboratory
Langley Field, Va.

CLASSIFICATION CANCELLED

Authority - NACA RF 2856 Date 12/20/54
By SA 12/20/54 See

Confidential
EO 10501 naca RF 2195
CLASSIFIED DOCUMENT

W. Crowley
JH-1-15-54

This document contains classified information affecting the national defense within the meaning of the Espionage Laws, Title 18, U.S.C. Sec. 793 and 794, and the transmission or the revelation of its contents in any manner to an unauthorized person is prohibited by law. Information so classified may be imparted only to persons in the military and naval services of the United States, appropriate civilian officers and employees of the Federal Government who have a legitimate interest therein, and to United States citizens of known loyalty and discretion who of necessity must be informed thereof.

**NATIONAL ADVISORY COMMITTEE
FOR AERONAUTICS**

WASHINGTON
April 13, 1948

UNCLASSIFIED

~~RESTRICTED~~
NACA LIBRARY
LANGLEY MEMORIAL AERONAUTICAL LABORATORY
CONFIDENTIAL

~~CONFIDENTIAL~~

UNCLASSIFIED

NACA RM No. L7112

~~CONFIDENTIAL~~
NATIONAL ADVISORY COMMITTEE FOR AERONAUTICS

RESEARCH MEMORANDUM

MEASUREMENTS OF THE WING AND TAIL LOADS

DURING THE ACCEPTANCE TESTS OF

BELL XS-1 RESEARCH AIRPLANE

By De E. Beeler and John P. Mayer

SUMMARY

Acceptance flight tests were conducted by the Bell Aircraft Corporation on the XS-1 research airplane to fulfill contractual requirements. During the tests, the NACA obtained preliminary measurements of the aerodynamic loads and handling qualities of the airplane. The maximum lift and buffet boundaries for the airplane were also determined. The buffet boundaries and the results of the load measurements for the airplane equipped with a 10-percent-thick wing and an 8-percent-thick tail are presented in this paper.

The results show that, except for a momentary increase between a Mach number of 0.57 and 0.65, the maximum lift decreases with increasing Mach number through the range of the tests. The maximum-lift values obtained during abrupt maneuvers were higher than those obtained during gradual maneuvers. Above a Mach number of 0.71, buffeting of the airplane was experienced before maximum lift was obtained.

The maneuvering and buffeting loads encountered at the high altitudes of the tests were well within the design loads for the wing and the horizontal tail up to maximum lift and to a Mach number of 0.80. The wing and the tail loads obtained in flight have shown fairly good agreement with wind-tunnel and calculated data.

It is indicated from the maximum lift and buffet boundary obtained up to a Mach number of 0.8 that an altitude of 30,000 to 40,000 feet would be an optimum altitude for proceeding to higher Mach numbers in the research program of the airplane.

INTRODUCTION

In connection with the NACA-Army flight-research program to obtain aerodynamic data at high speed, the Bell Aircraft Company

~~CONFIDENTIAL~~

UNCLASSIFIED

contracted to build a research airplane capable of attaining transonic speeds in level flight. During the acceptance tests of the airplane, the NACA obtained preliminary flight data which served as a guide in planning further flights at higher speeds and altitudes. The flight data were obtained from measurements of the loads acting on the airplane and from the determination of the stability and control characteristics of the airplane.

Reported herein are the results of the loads measurements together with the maximum lift and buffet boundaries for the airplane. Also included are applications of the data which may serve as guides in planning future flights of the airplane to higher speeds and altitudes.

The results of the stability and control measurements are reported in reference 1.

SYMBOLS

V_c	calibrated airspeed, miles per hour
q	free-stream dynamic pressure, pounds per square foot
p	static pressure, pounds per square foot
M	free-stream Mach number
n	normal load factor (measured perpendicular to airplane center line)
W	airplane gross weight, pounds
S	wing area, square feet
C_L	lift coefficient (Lift/ qS)
h_p	pressure altitude, feet
L	aerodynamic load, pounds
\bar{c}	wing mean aerodynamic chord, feet <i>4.5'</i>
M_0	airplane zero-lift pitching moment, tail off, foot-pounds
C_{m_0}	airplane zero-lift pitching-moment coefficient at low speed, tail off ($M_0/qS\bar{c}$)
g	acceleration of gravity, feet per second per second

x_t	horizontal distance from airplane center of gravity to tail quarter-chord station, feet = 40.5'
d	horizontal distance from wing-fuselage aerodynamic center to airplane center of gravity, feet 2.53'
x	horizontal distance from wing-fuselage aerodynamic center to tail quarter-chord station, feet $(x_t + d) 43.03'$
$1/\sqrt{1 - M^2}$	Glauert compressibility factor

Subscripts:

T	tail
A	airplane
F	fuselage
W	wing

DESCRIPTION OF THE AIRPLANE

The research airplane, designated by the Army as the XS-1, is a rocket-propelled straight-wing airplane. Although two models of the airplane were flown in the acceptance tests, one incorporating a 10-percent-thick wing and an 8-percent-thick horizontal stabilizer, and the other an 8-percent-thick wing and a 6-percent-thick horizontal stabilizer, the data presented herein were obtained with the 10-percent-thick wing airplane. Photographs of the airplane are given in figures 1 and 2, and a three-view drawing of the airplane is presented in figure 3. The dimensional characteristics of the airplane are listed in table I.

INSTRUMENTATION

Strain gages, used to measure shear and bending moment, were installed near the wing and tail root stations as indicated in figure 3. The shear gages were located on the front and rear spar webs near the neutral axis, and the bending-moment gages were located on the skin near the spar flanges. Calibrated loads were applied to the wing and the tail at various stations along the span and chord to make possible the interpretation of the measured strain-gage deflections in terms of applied loads. Strain-gage deflections were recorded on a 12-channel oscillograph. In addition to the recording oscillograph, standard

NACA instruments recording impact pressure, acceleration near the center of gravity, pressure altitude, and control positions were installed to aid in the evaluation of the measured-load data. The airspeed and altitude recorders were connected to a Kollsman fixed airspeed head located at approximately 100 percent of the local wing chord ahead of the wing near the wing tip.

TESTS

The flights were conducted by launching the XS-1 airplane from a modified bomb bay of a B-29 airplane at various altitudes. On completion of a powered flight, all fuel was jettisoned and a glide flight was made to landing. The tests were conducted at altitudes from 12,000 to 30,000 feet within a Mach number range of 0.27 and 0.80, and consisted of level-flight stalls, gradual turns to stall, and abrupt pull-ups to maximum obtainable lift and through the buffet boundary. The greater part of the data presented herein was obtained during gliding flight with all fuel jettisoned.

ACCURACY OF RESULTS

A preliminary calibration of the pitot-static installation on the XS-1 airplane was made up to a Mach number of 0.77. Results of the calibration indicated that, for these tests, the measured Mach number was accurate to ± 0.01 . Since the calibration showed that the position error was small, no correction for position error has been made in evaluating the Mach number. The measurement of tail and wing shear and bending moment is accurate to ± 100 pounds and ± 3000 inch-pounds, respectively, if errors which might be introduced by the recording oscillograph due to temperature and humidity changes are neglected. Due to errors introduced in the determination of wing loading, dynamic pressure, and the assumption that the lift is equal to the normal force, the maximum error in C_{L_A} is approximately ± 0.04 at the highest lift coefficients. At the lower lift coefficients encountered in high-speed flight the accuracy is better.

METHODS AND RESULTS

Time histories.— Typical time histories of various related quantities during abrupt pull-ups from level flight to stall and

during a gradual turn to stall are given in figures 4 and 5. The accelerations reported herein and used to determine airplane lift coefficient during buffeting have been obtained from a mean of the fluctuations of the acceleration record as indicated in figures 4 and 5. The wing and tail loads within the buffet region are mean values of the measured-load fluctuations. Due to the nature of the strain-gage records, however, these values were somewhat questionable. Except in the case of buffeting loads, therefore, the loads data presented in subsequent figures were obtained from points obtained below the buffeting boundary. The loads presented are measured values corrected for inertia loads and are therefore aerodynamic loads. The time histories presented in figures 4(b) and 5 for a Mach number of about 0.71 and 0.64, respectively, are representative of low-speed stalls; that is, the maximum lift possible in the particular maneuver is obtained before buffeting of the airplane occurs. The time histories of figure 4(a) are representative of a high-speed stall where buffeting occurs before maximum lift has been reached.

Maximum lift and buffet boundary.— Data were obtained up to Mach numbers of approximately 0.80 and from these data flight-test boundaries defining maximum lift and buffeting in terms of airplane lift coefficient and Mach number were established and are presented in figure 6. Boundaries are presented for abrupt maneuvers and gradual maneuvers. The abrupt maneuvers consisted of abrupt pull-ups, made as rapidly as possible, to stall. The gradual maneuvers are unaccelerated level-flight stalls and turns to stall. The boundaries have further been identified by appropriate symbols for the flight-test points to denote the attainment of buffeting at maximum lift and to denote the attainment of buffeting before maximum lift has been reached.

The Mach number range in which the maximum lift associated with a given maneuver is obtained before or simultaneously with the onset of buffeting is defined in this paper as the maximum-lift region. The Mach number range above 0.71 where buffeting occurs before maximum lift is reached regardless of the type of maneuver is defined as the buffet region. These regions are noted in figure 6. In the buffet region it may be noted that two boundaries are presented for the abrupt maneuver, one defining the first occurrence of buffeting, and one defining maximum lift obtained in the maneuver.

Airplane lift components.— Figure 7 shows the contribution of the wing, tail, and fuselage to the total airplane lift. The lift components are given in coefficient form and are based on the gross wing area. The components of lift due to the wing and tail have been determined from aerodynamic loads obtained from strain-gage measurements, while the lift due to the fuselage is the difference between the airplane total lift as determined by the normal acceleration, and the sum of the wing and tail lifts.

Tail loads.— In evaluating the tail load, flight conditions were chosen where the pitching acceleration was small or zero. With this selection, the tail load may be defined as

$$L_T = - \frac{C_{m_0} q S \bar{c}}{x \sqrt{1 - M^2}} + nW \frac{d}{x} \quad (1)$$

and may also be expressed as

$$\frac{L_T}{q \sqrt{1 - M^2}} = \frac{-C_{m_0} S \bar{c}}{x} + C_{L_A} \sqrt{1 - M^2} \frac{S d}{x} \quad (1a)$$

The flight data have been evaluated on the basis of equation (1a) and the results are shown in figure 8 where $\frac{L_T}{q \sqrt{1 - M^2}}$ is plotted against $C_{L_A} \sqrt{1 - M^2}$. The data apply specifically to the fuel-empty condition where the center of gravity and weight are constant. The slope of the line in figure 8 is, from equation (1a), a measure of the position of the aerodynamic center while the intercept is a measure of C_{m_0} . A curve derived from the results of wind-tunnel tests is also included for comparison. From the slopes and intercepts, the over-all low-speed coefficient C_{m_0} , the aerodynamic center for the tail-off condition, and the tail load per g, $\frac{Wd}{x}$, were determined for the flight and wind-tunnel data and are presented for comparison in table II.

Additional tail-load data were obtained during powered flights at various airplane gross weights. Since a direct record of fuel aboard was not obtained during flight, the weight at any instant was computed by using a value of the specific fuel consumption, determined from operational tests of the rocket on the ground, equal to 7.87 pounds of fuel mixture per second per cylinder. The center of gravity was computed by assuming a linear variation of the center-of-gravity position between the empty and full weight condition. The data for all weight conditions tested are included in figure 9, and the distance d is included in the parameter $C_{L_A} \sqrt{1 - M^2}$ to account for the various center-of-gravity positions associated with different airplane weights.

Wing lateral center of lift.— Figure 10 shows the variation of the lateral center of wing lift with wing lift coefficient. The lift center has been determined from shear- and bending-moment measurements by strain gages located approximately 4 inches outboard of the wing-fuselage junction. Therefore, the lateral center of lift as given is the centroid of the loading outboard of the gage station in terms of wing semispan. The data were obtained for Mach numbers ranging from 0.40 to 0.80. Included also in figure 10 are lateral-center-of-lift variations as computed by strip and the lifting-line theories. The locations of the centers of lift obtained by these methods are determined on the same basis as for the experimental data.

Buffeting loads.— During flights within the buffeting region, an envelope of wing- and tail-load fluctuations has been established and evaluated in terms of measured wing and tail buffeting loads. A variation of measured buffeting loads with airplane lift coefficient is presented in figure 11 for a range of Mach number from 0.72 to 0.80. The buffeting loads given in figure 11 are structural loads and include inertia effects.

DISCUSSION

Maximum lift and buffet boundary.— As is shown in figure 6, there is a general decrease in airplane maximum lift with increasing Mach number up to a Mach number of about 0.57. The maximum lift then increases until a peak is reached at a Mach number of 0.65 after which a general decrease in maximum lift continues with increasing Mach number. The peaking of the maximum-lift curve is characteristic of some low-drag airfoils where, for a small range of Mach numbers, the chordwise broadening of the low-pressure region more than offsets any reduction in negative pressure peaks that may occur with increasing Mach number. At higher Mach numbers the broadening of the low-pressure region is, in the present case, not sufficient to offset the reduction in negative pressure peaks, and the maximum lift continues to decrease with increasing Mach number.

The two points shown in figure 6 to the right of the vertical line and above the buffeting limit are believed to represent maximum lift coefficients. This belief is based on the fact that these two pull-ups were made as rapidly as possible and, as indicated in figure 4(a), a further movement of the elevator even after maximum lift had been obtained caused no further increase in acceleration. Although such behavior could also be attributed to a sudden increase in static stability or a loss in elevator effectiveness, the fact that these two points form a continuation of the solid curve to the left of a Mach number of 0.71 appears to substantiate the belief that these are maximum lift coefficients. Thus, the maximum-lift boundary for the

airplane appears to have been established up to a Mach number of approximately 0.8.

At Mach numbers greater than 0.71 airplane buffeting is experienced at lift coefficients less than maximum lift. These conditions are defined by the dashed buffet boundary in figure 6. Since the first indication of buffeting is a result of a partial breakdown of air flow over the wing, the buffet boundary does not necessarily represent a limiting boundary for the airplane. In order to attain maximum lift in the buffet region, the airplane must be flown through the boundary and into the buffet region.

In the maximum-lift region higher values of maximum lift were obtained for abrupt maneuvers than for gradual maneuvers. This effect is associated with the higher angular velocities in the abrupt pull-ups. Sufficient data have not been obtained to establish the effect of angular velocity on maximum lift.

Airplane lift components.— It is shown in figure 7 that the fuselage of the XS-1 airplane produces approximately 20 percent of the total lift of the airplane at the higher lift coefficients. Since the area intercepted by the fuselage is about 20 percent of the wing area, it is seen that the fuselage carries load corresponding approximately to the intercepted wing area. Within the range of the tests it appears that any Mach number effect on the distribution of lift between the components is small.

Horizontal-tail loads.— From the results given in figures 8 and 9 and the comparisons of the derived quantities shown in table II, it can be seen that there is good agreement between the flight and wind-tunnel values for the aerodynamic center, and the tail load per g, and reasonable agreement for the pitching-moment coefficient of the wing-fuselage combination. Within the range tested, the loads on the tail are considerably less than the design values, since the airplane was designed initially for a moment coefficient of -0.1 , and the horizontal tail was designed to withstand the load required to balance $18g$ at a weight of 8400 pounds.

Wing lateral center of lift.— From the results given in figure 10 it can be seen that the wing lateral center of pressure is constant at the higher wing lift coefficients but, due to a slight washout of the wing, moves inboard a very small amount at lower lift coefficients. It is also seen that the measured results agree very well with predicted values obtained from either lifting-line or strip theory. It may be inferred from the small amount of scatter that the effect of Mach number on the center of pressure is negligible in the range from 0.3 to 0.8.

Wing and tail buffeting loads.— Sufficient data were not obtained during the acceptance tests of the airplane to determine the variation of buffeting loads with Mach number. However, it is shown (fig. 12) that there is an increase in wing and tail buffeting loads with an increase in airplane lift coefficient. Buffeting frequencies of approximately 14, 25, and 40 cycles per second have been established from the strain-gage records. The first two values correspond roughly to the wing and tail first symmetrical bending modes of vibration. There is no apparent effect of Mach number and lift coefficient on the observed frequencies. The magnitude of the buffeting loads for the Mach number and lift-coefficient range tested is relatively low and is well within design-load limits of the airplane.

Load factor and altitude limit boundaries.— Although the flights on the XS-1 reported herein have not given rise to particularly severe loads or unexpected Mach number effects, it is desirable in extending the program to carry out future tests at altitudes as high as possible in order to both minimize the impact pressure for a given Mach number and to limit the amount of load which may inadvertently be placed on the airplanes. The upper boundary given in figure 6 together with the relation

$$n = \frac{0.7\rho M^2 C_{L_A}}{W/S}$$

has been used to derive the curves given in figure 12. The two wing loadings shown correspond to the fully loaded condition and to the condition where approximately 1 minute of fuel remains. The load-

factor relation $n = \frac{0.7\rho M^2 C_{L_A}}{W/S}$ has also been used to determine the

maximum altitude at which 1g level flight is possible at various Mach numbers. These results are shown in figure 13 for the same two wing loadings.

The results shown in figure 13 constitute an upper limit of altitude for level-flight operation with no margin for maneuvering. The lower altitude limit for operation may be obtained from figure 12 and is determined by the selection of the margin of maneuverability required to perform the tests. Assuming that a 1g margin is required for maneuvering, it appears on the basis of these limits that the optimum operating altitude for future tests would be between 30,000 and 40,000 feet, the lower limit being associated with the higher wing loading.

CONCLUSIONS

From the data obtained during the acceptance tests of the XS-1 research airplane, it is shown that:

1. The maximum lift obtained in abrupt maneuvers decreases with an increase in Mach number up to a Mach number of 0.80 with the exception of a minor increase in lift between a Mach number of 0.57 and 0.65.

2. The variation of maximum lift obtained in gradual maneuvers with Mach number indicated the same trend as in abrupt maneuvers, except that maximum-lift values obtained in abrupt maneuvers were higher than those obtained in gradual maneuvers.

3. The wing and tail-load data have shown fairly good agreement with wind-tunnel and calculated data.

4. The loads encountered up to maximum lift and to a Mach number of 0.80 are well within the design conditions for the wing and horizontal tail.

5. The optimum altitude for proceeding to higher Mach numbers in the research program of the airplane appears to be between 30,000 and 40,000 feet.

Langley Memorial Aeronautical Laboratory
National Advisory Committee for Aeronautics
Langley Field, Va.

REFERENCE

1. Williams, Walter C., Forsyth, Charles M., and Brown, Beverly, P.:
General Handling-Quality Results Obtained during Acceptance
Flight Tests of the Bell XS-1 Airplane. NACA RM No. L8A09,
1947.

TABLE I.— DIMENSIONAL CHARACTERISTICS
OF XS-1 AIRPLANE

Airplane:

Weight during acceptance tests:	
Landing condition (no fuel), lb	6750
Launching condition (full fuel), lb	12,000
Center-of-gravity position, percent mean aerodynamic chord:	
Landing condition (no fuel)	25.3
Launching condition (full fuel)	22.4
Horizontal distance from airplane center of gravity to tail quarter-chord station (c.g. 25.3 percent), ft.	13.313

Power plant of rocket motor:

Number of cylinders	4
Static thrust (each cylinder), lb	1500

Wing:

Area, sq ft (including section through fuselage)	130
Span, ft	28
Airfoil section (root to tip)	NACA 65 ₁ -110(a = 1)
Thickness (percent wing chord)	10
Aspect ratio	6
Taper ratio	2:1
Mean aerodynamic chord, in.	57.71
Incidence root chord, deg	2.5
Geometric twist, deg	1° washout root to tip
Sweepback (leading edge), deg	5.05
Dihedral, deg	0

Horizontal tail:

Area, sq ft	26.0
Thickness, percent chord	8.0
Span, ft	11.4
Aspect ratio	5.0

Elevator:

Area, sq ft	5.2
Travel relative to stabilizer, deg	15 up, 10 down
Chord, percent of horizontal-tail chord	20

TABLE II.— COMPARISON OF FLIGHT AND WIND-TUNNEL
RESULTS FOR THE XS-1 AIRPLANE

Source of tests	Location of airplane aerodynamic center, tail off, percent M.A.C.	Horizontal tail load per g (a)	Over-all pitching-moment coefficient for wing-fuselage combination
Flight	8.1	395	-0.06
Wind tunnel	6.9	422	-.05

^aAirplane c.g. at 25.3 percent M.A.C.; W = 6750.

NATIONAL ADVISORY
COMMITTEE FOR AERONAUTICS

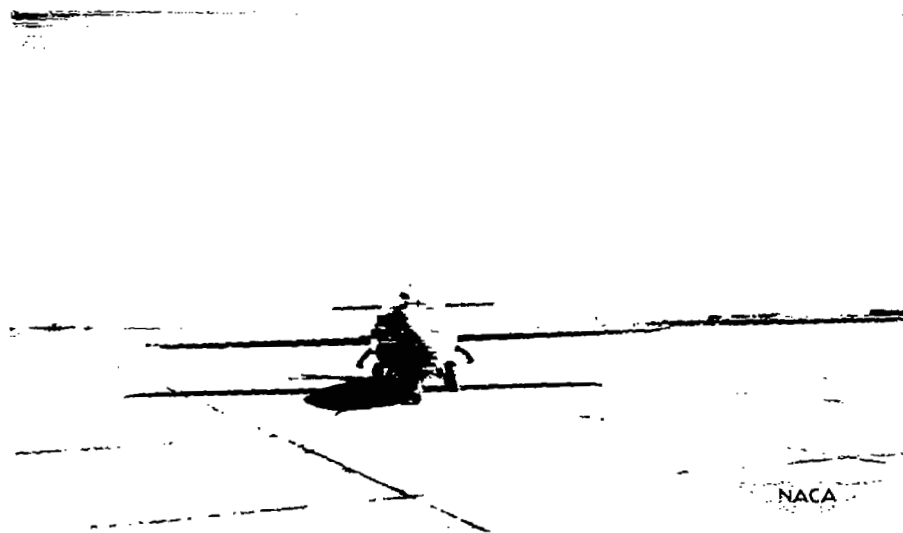


Figure 1.- Front view of the XS-1 airplane.

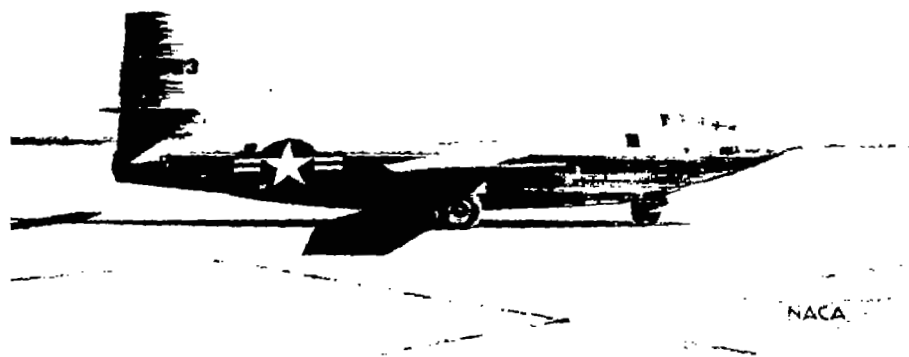
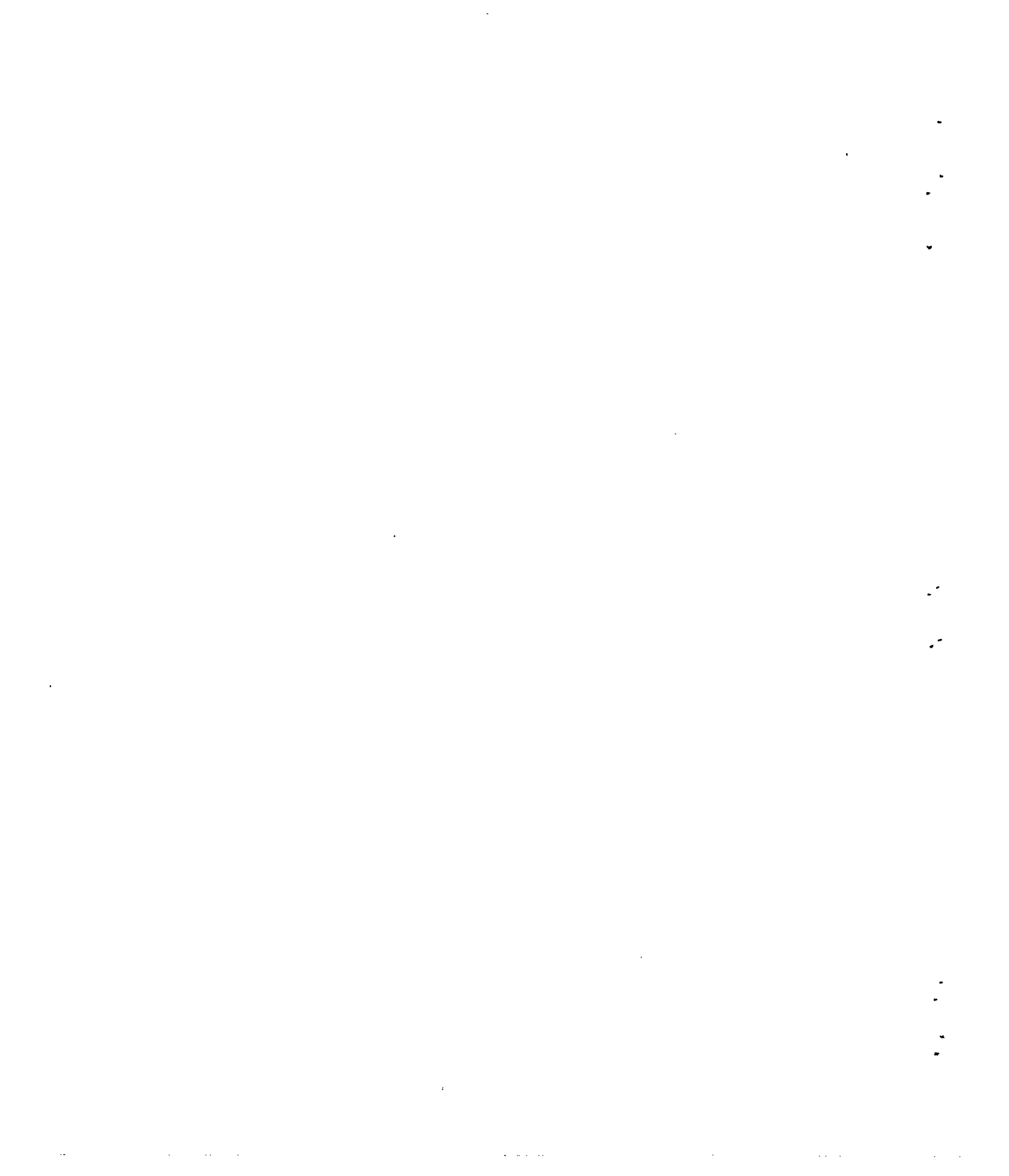


Figure 2.- Side view of the XS-1 airplane.





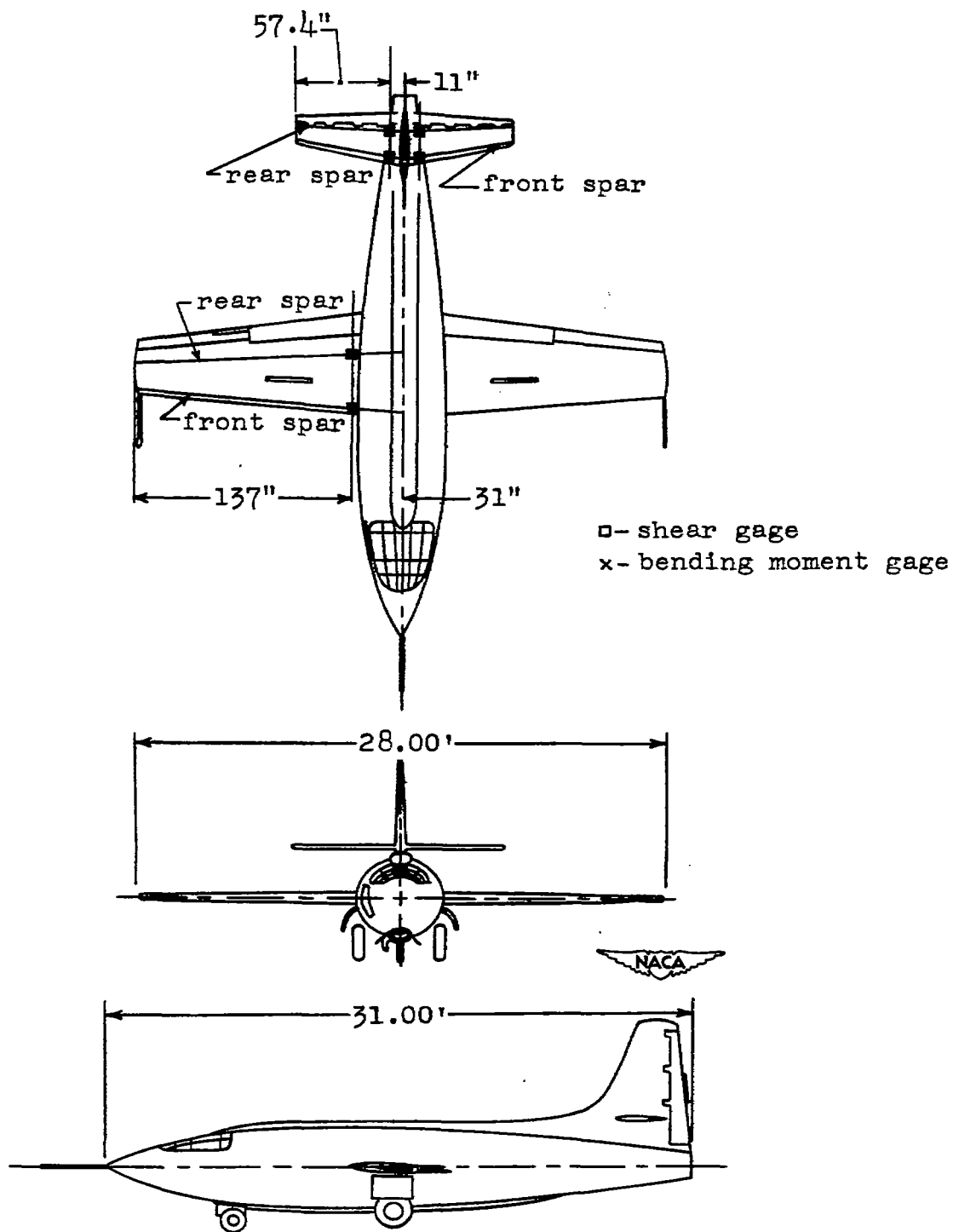


Figure 3.- Three-view drawing of XS-1 airplane showing location of strain gages for measuring wing and tail loads.

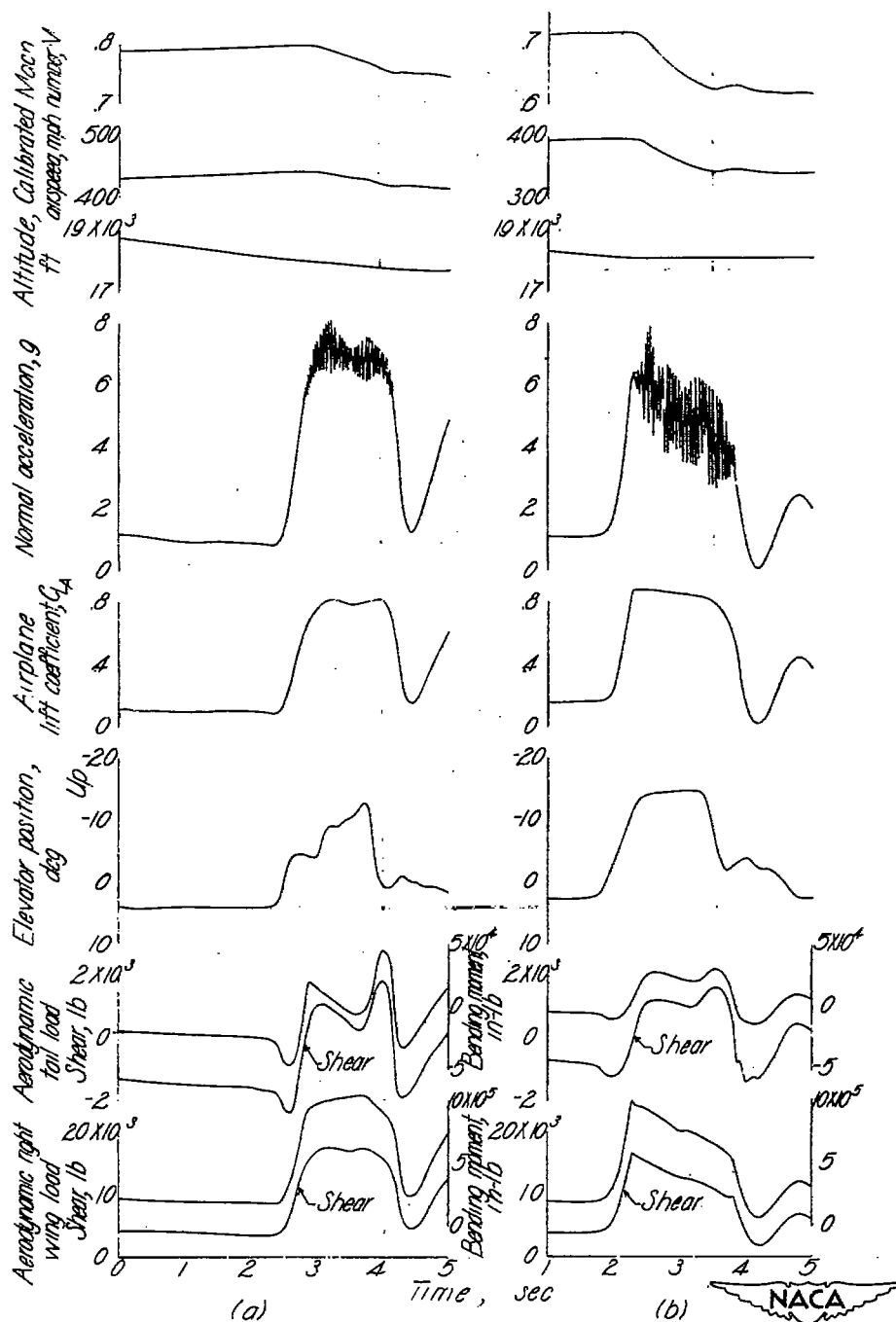


Figure 4. - Typical time histories of measured quantities during an abrupt pull-up (a) through the buffet boundary (b) to maximum lift coefficient. Fuel-empty condition. X-5 airplane. Ten-percent-thick wing.

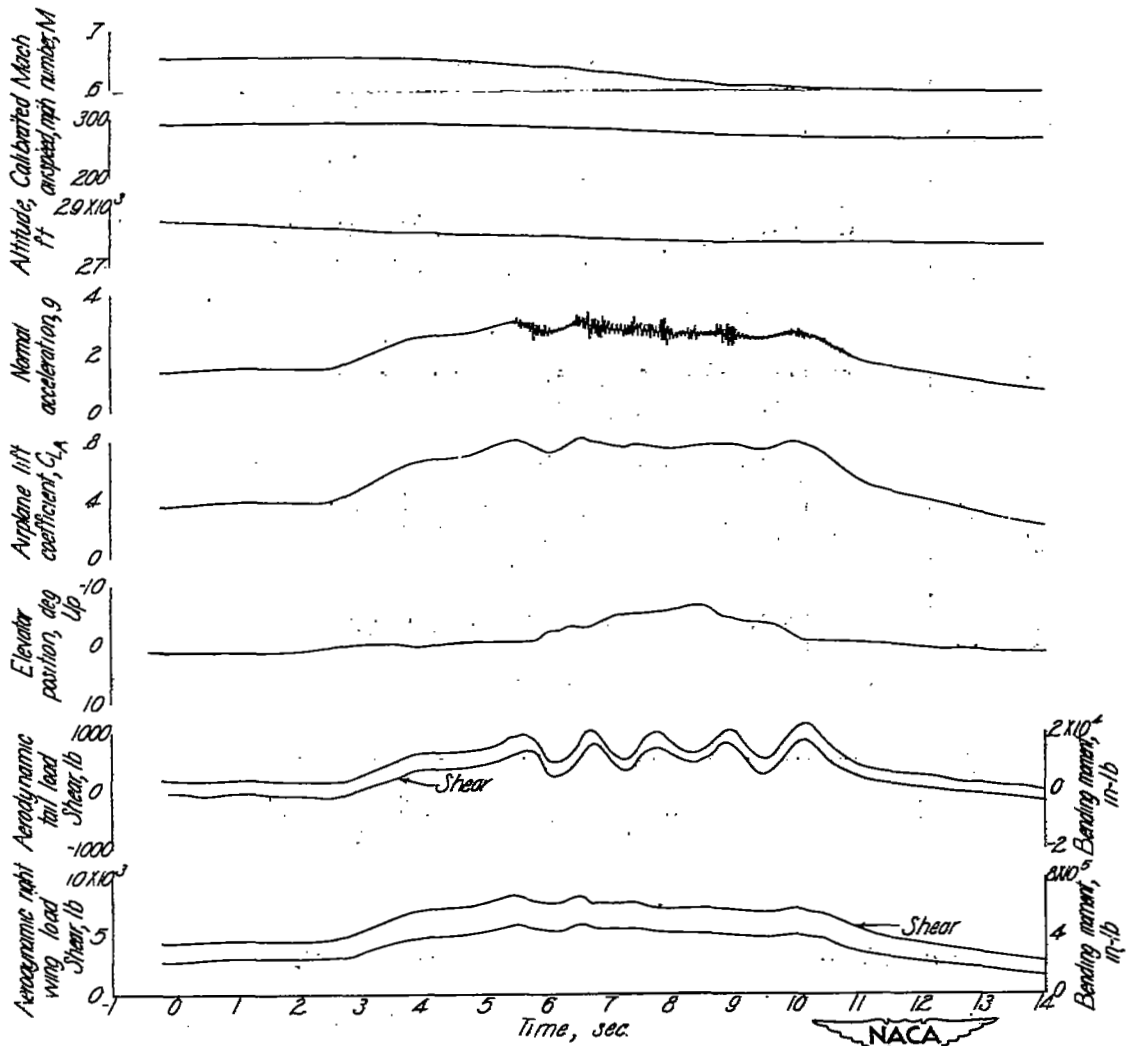


Figure 5 - Typical time history of measured quantities during a gradual turn to maximum lift Fuel-empty condition. XS-1 airplane. Ten-percent-thick wing.

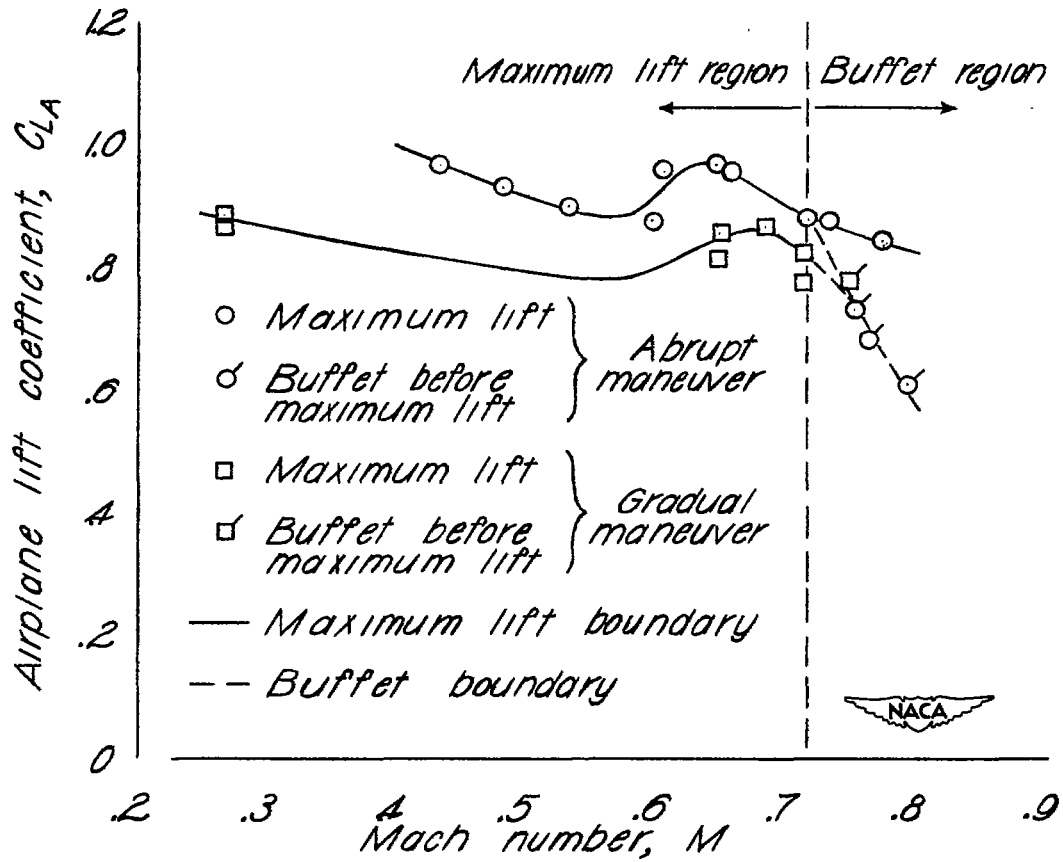


Figure 6. - Maximum lift and buffet boundaries.
XS-1 airplane. Ten-percent-thick wing.

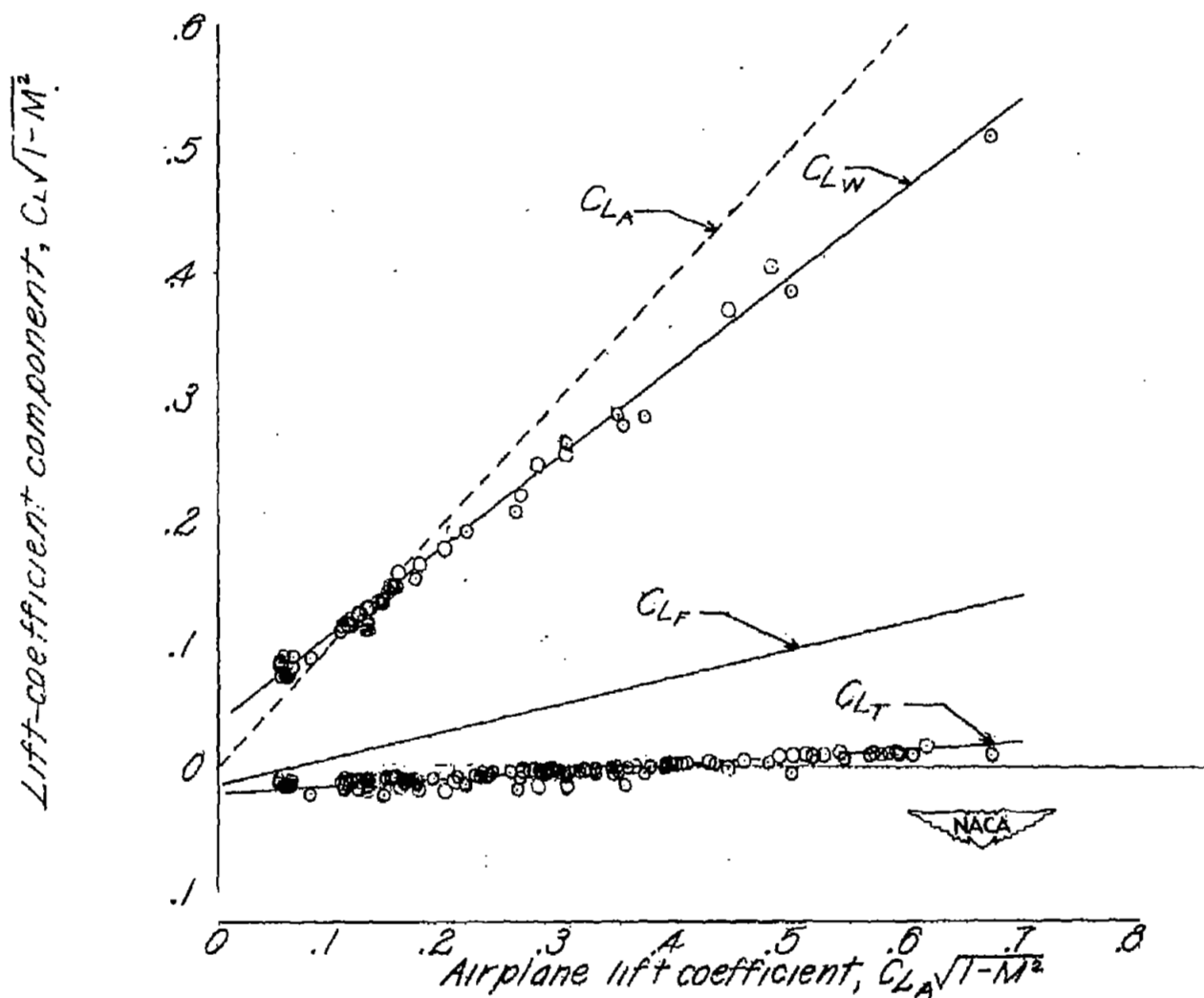


Figure 7. — Components of lift coefficient due to wing, tail, and fuselage. X-51 airplane. Ten-percent-thick wing.

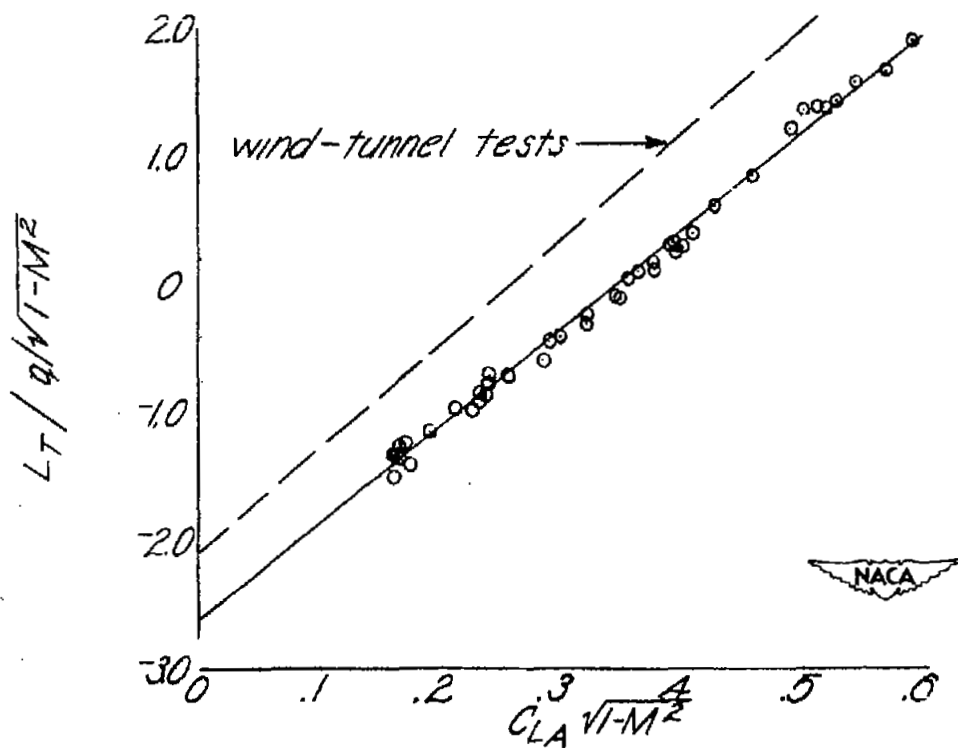


Figure 8.— Variation of the horizontal tail load with airplane lift coefficient during gradual turns. XS-1 airplane. Ten-percent-thick wing. Fuel-empty condition.

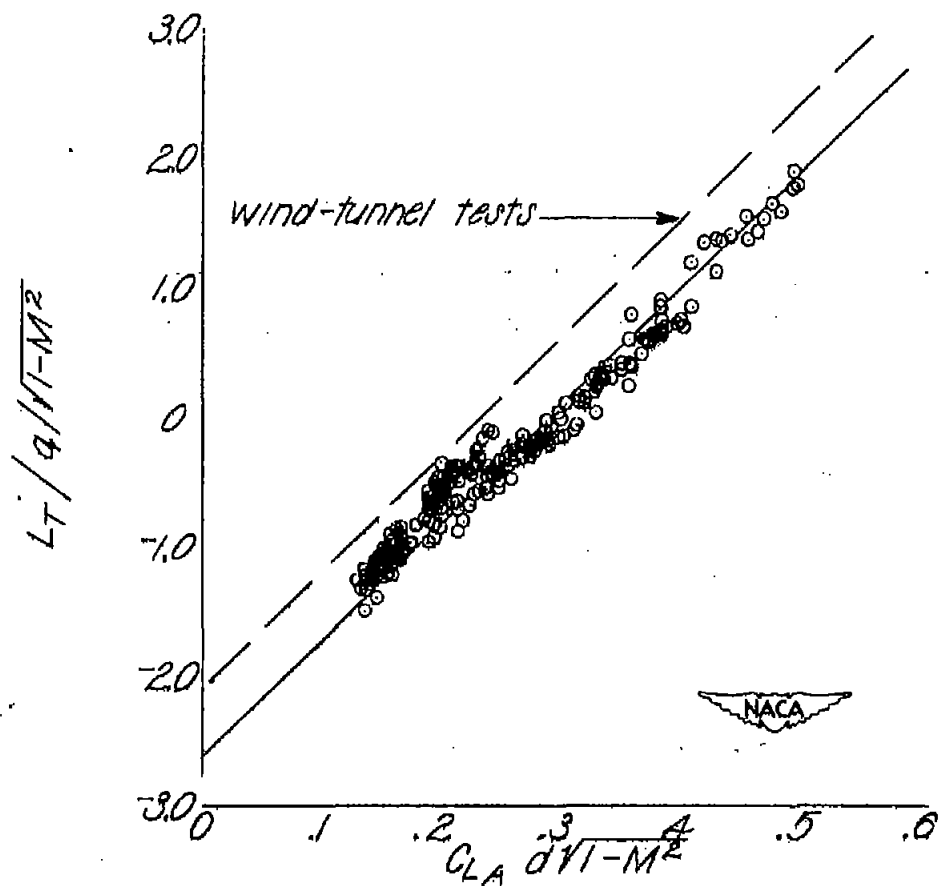


Figure 9.—Variation of the horizontal tail load with airplane lift coefficient during gradual turns of various wing loadings. XS-1 airplane. Ten-percent-thick wing.

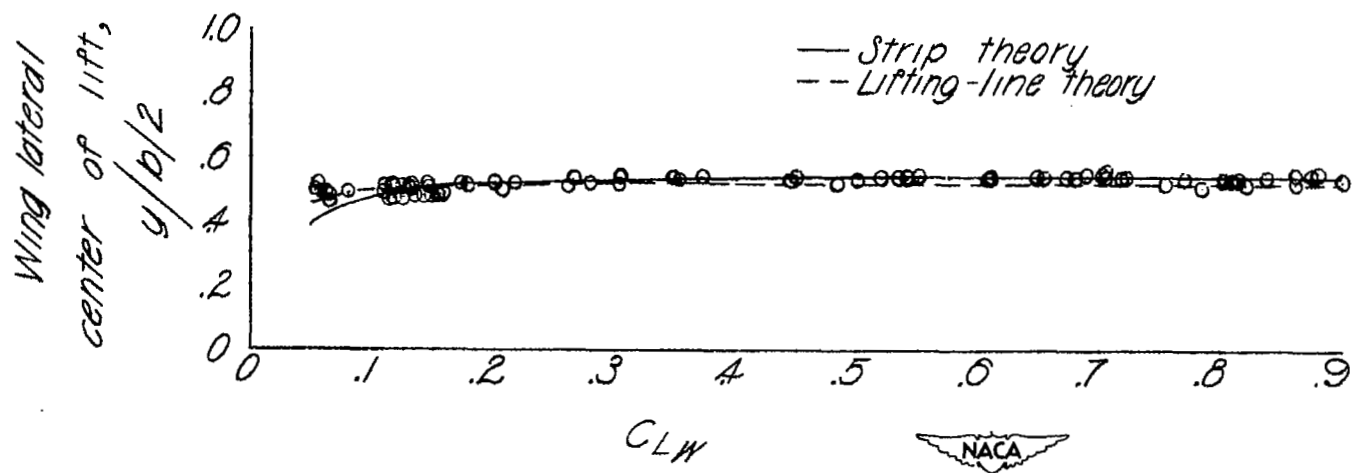


Figure 10. — Variation of measured lateral center of lift of the right wing with wing lift coefficient. XS-1 airplane. Ten-percent-thick wing. Mach number range 0.3 to 0.8.

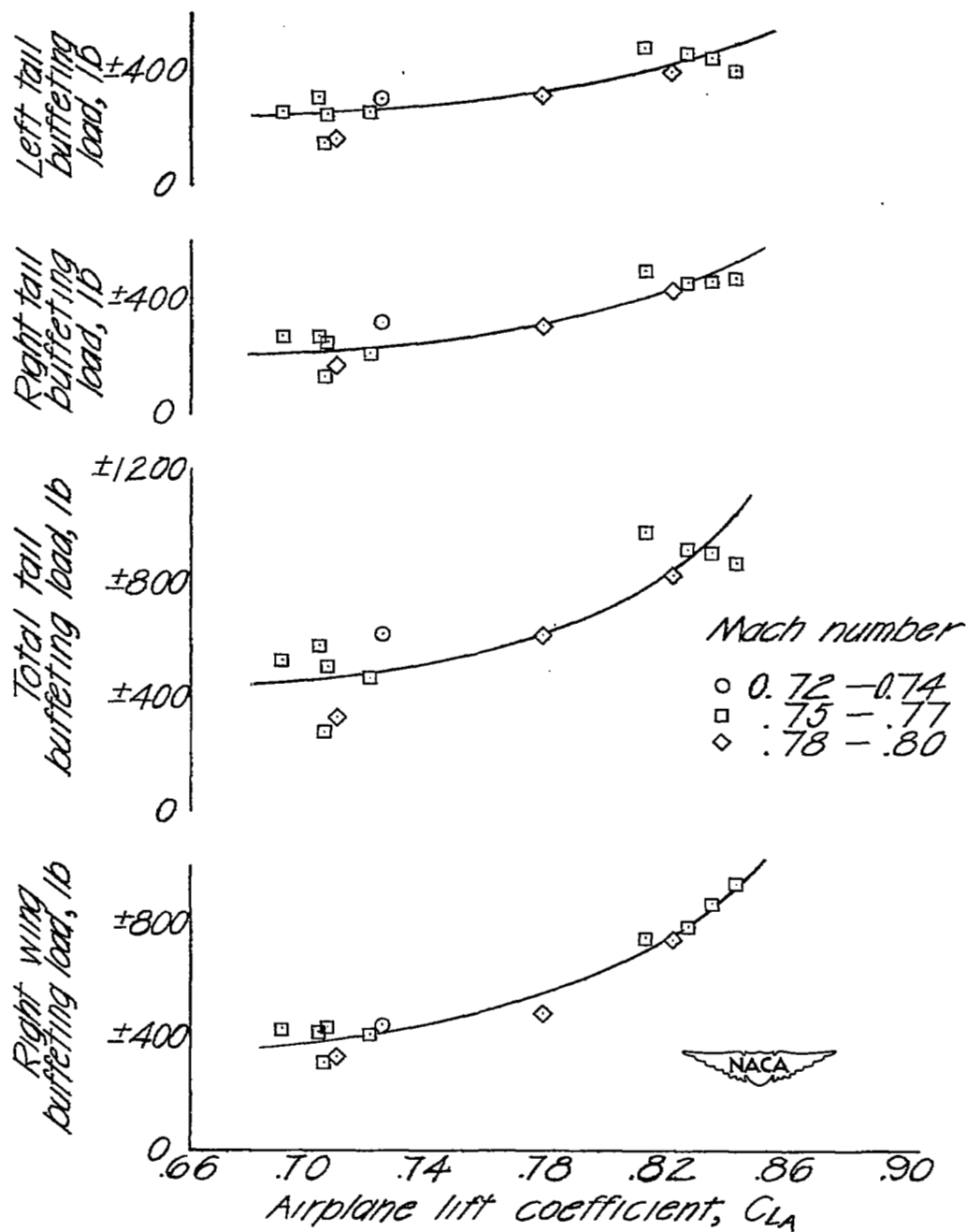


Figure 11.— Variation of measured wing and tail buffeting loads with airplane lift coefficient. XS-1 airplane. Ten-percent-thick wing.

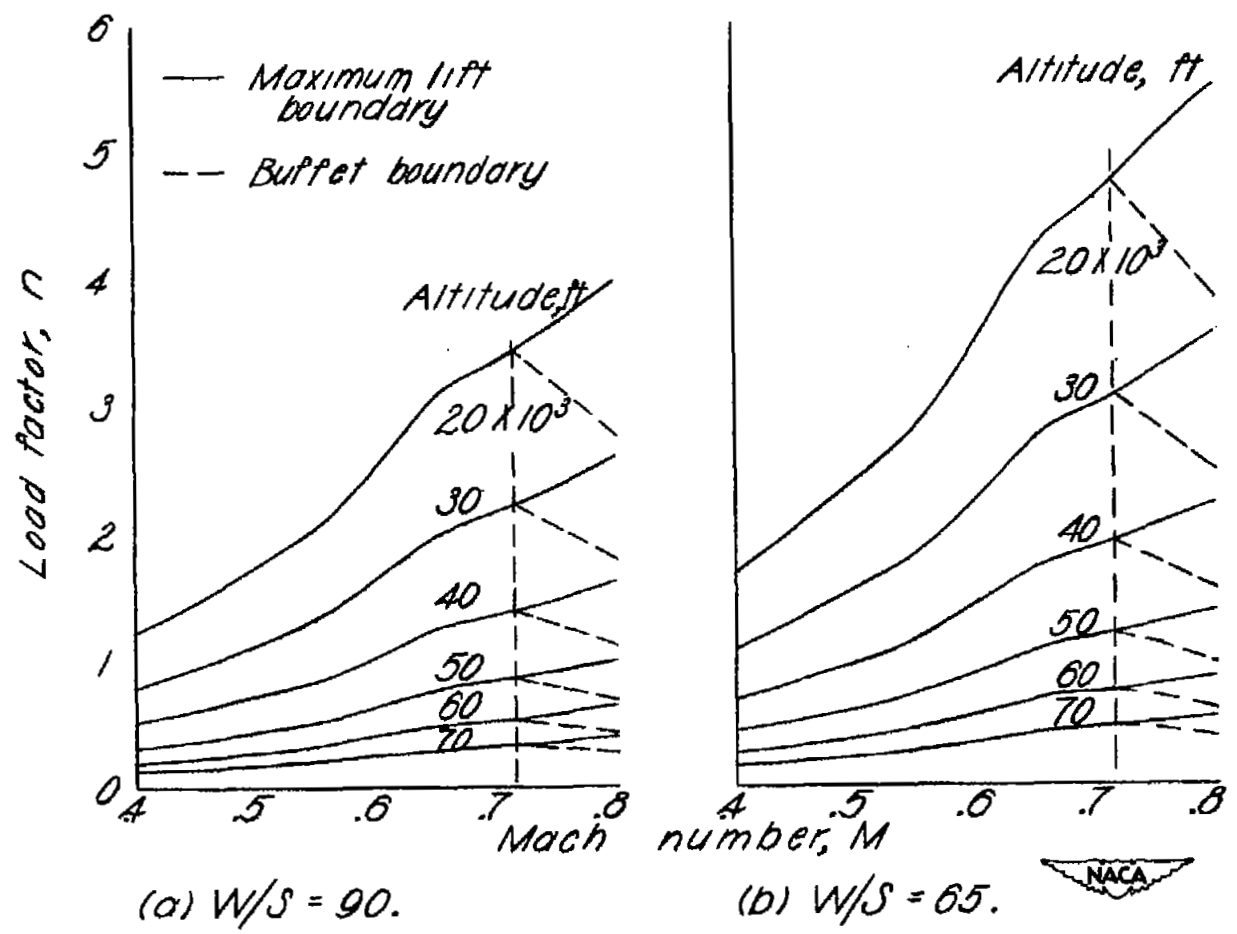


Figure 12. - Load-factor boundaries for the X-1 airplane.
 Ten-percent-thick wing.



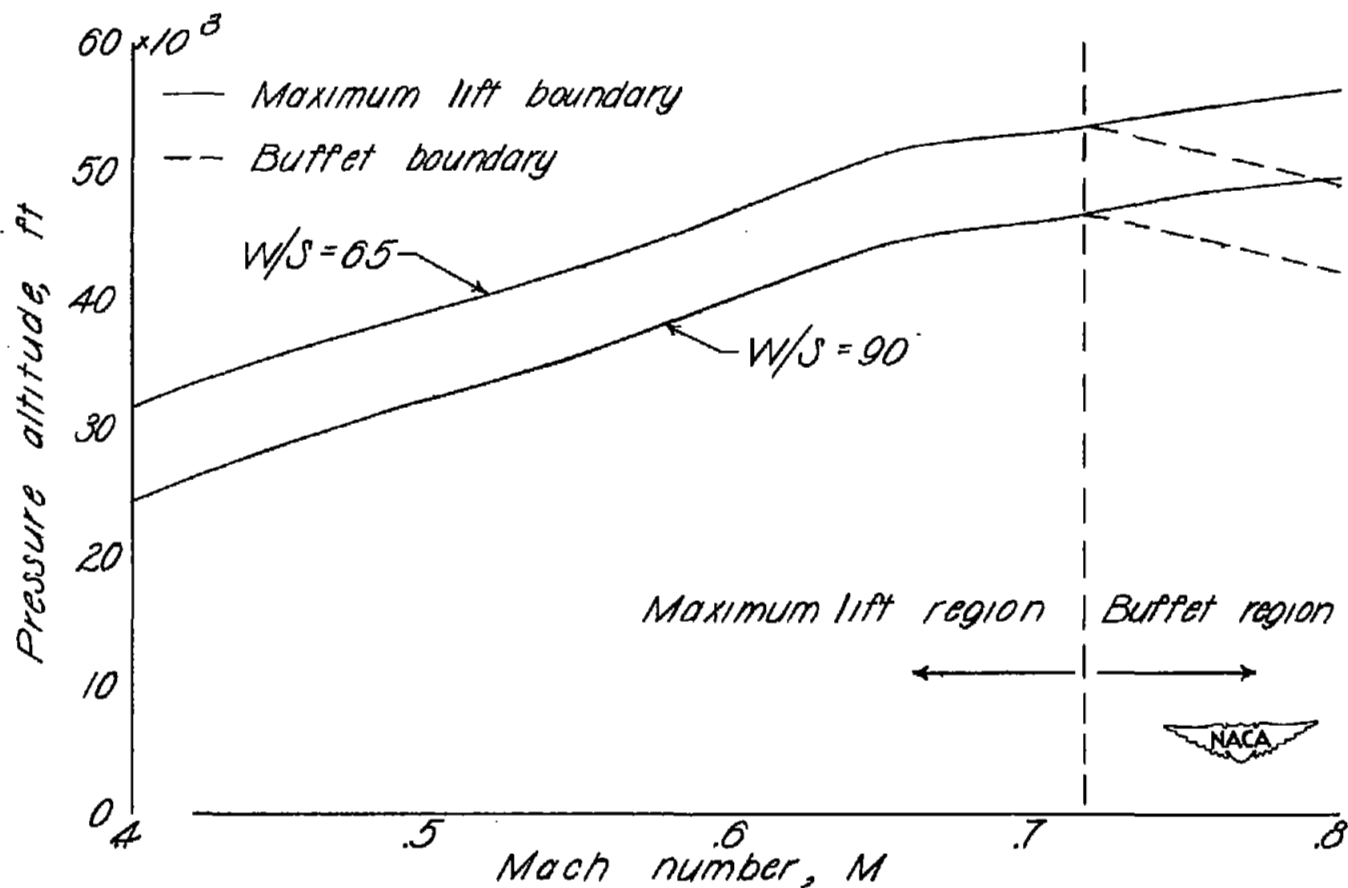


Figure 13.—Altitude boundaries for the X-1 airplane flying at a load factor of 1. Ten-percent-thick wing.